

Measurement of the high energy contribution to Gerasimov-Drell-Hearn sum rule

June 5, 2019

A. Deur

Thomas Jefferson National Accelerator Facility, Newport News, VA 23606, USA

S. Širca

University of Ljubljana, Ljubljana, Slovenia

J. Stevens

College of William and Mary, Williamsburg, Virginia 23187-8795, USA

Abstract

We propose to measure the high-energy behavior of the integrand of the Gerasimov-Drell-Hearn (GDH) sum rule, i.e. the doubly polarized total photoproduction cross-section asymmetry. The high-energy domain is where a failure of the GDH sum rule could occur, due to either a non-vanishing of the polarized Compton Amplitude, or a diverging or too slow convergence of the GDH integrand. Such behavior would reveal new nucleon structural processes. Independent of the sum rule study, the measurement will constrain our knowledge of QCD in a domain where its phenomenology is unknown, when spin degrees of freedom are explicit. In particular it will clarify a discrepancy between fits of the photoproduction and DIS world data and theoretical expectation, which predicts an opposite sign of high-energy behavior of the GDH integrand. Chiral perturbation theory will also be tested in a different regime than that covered by the low Q^2 JLab spin sum rule program. These measurements provide would a baseline for the EIC's study of the transition between polarized DIS and the polarized diffractive regime. In addition, the experiment should also be sensitive enough to provide for the first time a non-zero deuteron asymmetry in the diffractive regime, and would also constrain the polarizability contribution to the muonic hydrogen hyperfine splitting. In this Letter of Intent (LOI), we propose to perform the measurement on the proton and neutron in Hall D, which is especially suited for such measurement thanks to its high-energy tagged photon beam, high-luminosity and large solid angle detector.

Contents

1	Motivation	4
1.1	The Gerasimov-Drell-Hearn Sum Rule	4
1.2	Experimental Status	7
2	Experimental strategy and set-up	7
2.1	Beam	8
2.2	Target	10
2.3	FROST target characteristics	10
2.4	Detectors and acquisition	12
3	Sensitivity and beam time request	12
3.1	Uncertainties	13

4	Impact of the results	17
4.1	Determination of the real and imaginary parts of the spin-dependent Compton amplitude $f_2(\nu)$	17
4.2	The intercept of the a_1 Regge trajectory	20
4.3	Deuteron asymmetry	21
4.4	Polarizability correction to hyperfine splitting in muonic hydrogen	21
4.5	Transition between polarized DIS to diffractive regimes	23
4.6	Constraint on quark compositeness or size	24
5	Summary	26

1 Motivation

1.1 The Gerasimov-Drell-Hearn Sum Rule

The Gerasimov-Drell-Hearn (GDH) sum rule [1] is a general and fundamental relation that links the anomalous magnetic moment κ of a particle to its helicity-dependent photoproduction cross sections:

$$I = \int_{\nu_0}^{\infty} \frac{\Delta\sigma(\nu)}{\nu} d\nu = \frac{4\pi^2 S \alpha \kappa^2}{M^2}, \quad (1)$$

where ν is the probing photon energy, ν_0 is the photoproduction threshold, S is the spin of the particle, M is its mass, and α the QED coupling. $\Delta\sigma \equiv \sigma_P - \sigma_A$ where σ_P and σ_A denote the photoproduction cross sections for which the photon spin is parallel and antiparallel to the target particle spin, respectively. The sum rule is valid for any type of target particles, from photons or electrons, to the nucleon or nuclei. For the proton, $S = 1/2$ and $I^p = 204.8(0) \mu\text{b}$, but for a structureless ($\kappa = 0$) particle, the sum rule holds at each order in perturbation theory.

Several methods have been used to derive the GDH sum rule using dispersion relations or current algebra in the form-front or in the light-front [2, 3]. The derivation assumes cornerstones of quantum field theory: causality (dispersion relation), unitarity, Lorentz and gauge invariances (low energy theorem), as well as a "no-subtraction hypothesis". It assumes a good ν convergence of the spin-dependent Compton amplitude and thus depends on the target studied. For example for an electron target, QED calculations show the amplitude converges fast enough and the GDH sum rule is verified on the electron. However, there has been much discussion on whether the no-subtraction hypothesis holds in the context of the nucleon GDH sum rule, see e.g. Ref. [4].

Equation (1) reveals that the excitation spectrum of composite particles is related to their non-zero κ . The saturation of the sum rule beyond a given ν indicates the energy scale at which the object structure or mass scales become irrelevant. For examples, for a lepton l at first order in perturbation, $\Delta\sigma(\nu)$ is non-zero only around the lepton mass [3] (where it switches sign to insure that $I^l = 0$); for a nucleon only a single quark participates in the reaction at high energies and, if quarks are structureless, $\kappa_q = 0$ for the active quark thus it does not contribute to the sum rule.

Therefore, while the nucleon GDH sum gets most of its contribution from resonances, the high-energy part is equally important since it may reveal possible substructure or unknown structural processes. Inspection of the sum rule derivation shows that it is the high energy domain that would likely expose a failure of the sum rule. In fact,

the unpolarized equivalent of the GDH sum rule diverges, for both nucleons, due to the behavior of its integrand at high- ν . As shown in Fig. 1, the divergence in the unpolarized cross section only becomes clear from high- ν data, $\nu > 3$ GeV. This high-energy regime is not probed by current GDH integrand measurements, underlining the need for the high- ν measurements proposed here. Furthermore, clearly one needs to be well away from resonance bumps to efficiently fit $\Delta\sigma(\nu)$, e.g. with a Regge-based form, in order to assess its behavior when $\nu \rightarrow \infty$.

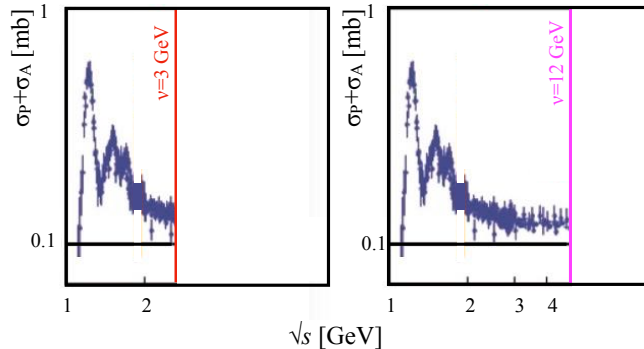


Figure 1: Unpolarized total photoabsorption cross-section $\sigma_P + \sigma_A$ for the proton, vs Mandelstam \sqrt{s} (log scale). Left panel: the red line marks the current highest \sqrt{s} at which the GDH integrand $\Delta\sigma$ has been measured. There would be no sign of potential divergence for the unpolarized equivalent of the GDH sum rule, $\int \sigma_P + \sigma_A d\nu$, if its measurement had stopped at this limit. Right panel: the magenta line indicates the highest \sqrt{s} reachable in Hall D. The convergence problem for $\int \sigma_P + \sigma_A d\nu$ is clear. Plots after Ref. [5].

Possible causes for a GDH sum rule violation are reviewed in [3]. The ones most considered are A) the existence of quark substructure (non-zero quark anomalous moments) just discussed [7]; B) The existence of a $J = 1$ pole of the nucleon Compton amplitude [8]; and C) the chiral anomaly [9]. All proposed mechanisms would manifest themselves at high- ν . Since there is no low- ν mechanism that could invalidate the sum rule and since its convergence can be investigated only beyond the resonance region, to truly verify the sum rule, the behavior of $\Delta\sigma$ at high- ν must be measured.

It is beneficial to measure $\Delta\sigma$ on both nucleons, to allow for an isospin analysis of their high- ν behavior. To quote the review [10]:

... above the resonance region, one usually invokes Regge phenomenology to argue that the integral converges [...] However, these ideas have still to be tested experimentally. [...] the real photon is essentially absorbed by coherent processes, which require interactions among the constituents such as gluon

exchange between two quarks. This behavior differs from DIS, which refers to incoherent scattering off the constituents.

Regge theory suggests that at high ν , $\sigma \equiv \sigma_P + \sigma_A$ is determined by the Pomeron-trajectory, while $\Delta\sigma(\nu) \propto (\nu + M/2)^{\alpha_0-1}$ [18], with α_0 a Regge intercept. For the isovector part of $\Delta\sigma^{p-n}$, α_0 should be determined by the $a_1(1260)$ meson trajectory, which is still not well known. For the isoscalar $\Delta\sigma^{p+n}$ part, α_0 should be given by the $f_1(1285)$, which is better known. Interestingly, this isoscalar part of $\Delta\sigma$ is presently assumed to be zero in most analyses since a non-zero deuteron asymmetry remains to be measured in the diffractive regime [11, 12]. Thus, a completed and accurate analysis necessitates measurements for both the proton and neutron and this experiment will be precise enough to measure clearly and for the first time a non-zero polarized deuteron signal in this regime.

Beyond the sum rule study, the measurement will investigate QCD in its diffractive scattering regime, where Regge theory is expected to describe the scattering process. As signaled in the Review [10] and quoted above, this phenomenology is not tested with spin degrees of freedom, an important shortcoming, as emphasized by Bjorken [15]: *“Polarization data has often been the graveyard of fashionable theories. If theorists had their way, they might well ban such measurements altogether out of self-protection.”* This seems supported by the stark discrepancy discussed in Section 4.2 between fits of the photoproduction and DIS world data and Regge theory’s expectation.

Dispersion theoretic analysis of $\Delta\sigma(\nu)$ will yield the complex spin-dependent Compton amplitude $f_2(\nu)$ (see next section and Section 4.1), and thereby offers a test of Chiral effective field theory (χ EFT), the leading non-perturbative approach to QCD at low energy-momentum. This will complement the JLab low Q^2 spin sum rule experimental program that tested χ EFT and showed that description of spin observables are challenging for χ EFT [6].

Finally, measuring $\Delta\sigma(\nu)$ will provide a baseline for some of the Electron Ion Collider (EIC) studies, as well as constraint of the polarizability contribution to the muonic hydrogen hyperfine splitting, see Section 4.4 and Section 4.5.

The GDH sum rule and its generalization have been the objects of active experimental programs at BNL, ELSA, ESRF, JLAB, MAMI, SLAC and TUNL, see Refs. [2, 6] for reviews, where $\Delta\sigma(\nu)$ was measured up to 2.9 GeV. This document proposes to use the polarized 12 GeV CEBAF beam to measure the high-energy behavior of the GDH sum on the proton and neutron. Hall D, with its high-luminosity photon tagger and its large solid angle detector is well-suited for such an experiment. We plan to first measure the

yield difference $\Delta y(\nu) \propto \Delta\sigma(\nu)$ since it is sufficient to study the integral convergence. This eliminates uncertainties coming from normalization factors and from unpolarized backgrounds. The other goals of this LOI require absolute normalization of $\Delta\sigma(\nu)$. The measurement would extend by a factor of 4 the experimental integration range. It will cover the domain relevant to clarify the question of the convergence of the GDH sum while probing for unknown parton process or structure since studying the anomalous magnetic moment is a (relatively) low-energy but powerful probe of compositeness: the discovery that $\kappa_p \neq 0$ in the 1930s [13] gave a first evidence for the proton's composite structure, well before form factor measurements at higher energies [14].

1.2 Experimental Status

The GDH integrand for the proton was measured at LEGS (BNL), MAMI and ELSA. The LEGS measurement spans $0.2 \leq \nu \leq 0.42$ GeV and yields a π^0 contribution to I of $125.4 \pm 1.7 \pm 4.0$ μb [20]. The MAMI measurement covers $0.2 \leq \nu \leq 0.8$ GeV and yields a contribution of $254 \pm 5 \pm 12$ μb , The ELSA measurement covers $0.7 \leq \nu \leq 2.9$ GeV and yields a contribution of $48.3 \pm 2.5 \pm 2.1$ μb [21]. It was shown that a Regge behavior is adequate down to $\nu \approx 1.2$ GeV [2]. Assuming a Regge parameterization for the $\nu > 2.9$ GeV extrapolation yields a 14 μb contribution. The $\nu = 0.14$ to 0.2 GeV contribution is estimated at 28 μb by the MAID parameterization [22]. In all, these measurements/estimates yield $I = 208 \pm 6 \pm 14$ μb using the LEGS data at low ν , or $I = 212 \pm 6 \pm 16$ μb using the low ν MAMI data and MAID. This agrees with the GDH prediction $I^p = 204.8$ μb with a 10% accuracy.

An experiment with similar goals as that of the LOI, E159 [16], was approved at SLAC but did not run due to the End Station A program termination. Another real photon GDH experiment [17] was approved at JLab with A⁻ rating but did not run due to delay in the polarized HD target availability and the termination of the 6 GeV program.

2 Experimental strategy and set-up

We propose to focus primarily on measuring the yield difference $\Delta y(\nu) = N^+ - N^-$ (where $N^{+(-)}$ is the number of events in a bin ν for positive (negative) beam helicity), rather than the absolute $\Delta\sigma$. This eliminates uncertainties coming from normalization factors, such as polarimetry uncertainties, which are typically dominant in experiments

measuring polarized cross sections. Furthermore, uncertainties from unpolarized contributions (target dilution) cancel in the $N^+ - N^-$ difference.

Measuring $\Delta y(\nu)$ is sufficient to establish the convergence of the GDH integral. Normalizing $\Delta y(\nu)$ into a cross section *via* the beam flux, target density, solid angle, beam polarization, target polarization, and efficiencies, is of secondary importance. This is because only the ν -dependence of $\Delta\sigma$ is necessary to assess the convergence of the integral since for it to converge¹, $|\Delta\sigma/\nu|$ must decrease with ν . This is not the case for $|\sigma/\nu|$ and as described in Sec. 1.1 the equivalent of the unpolarized GDH sum does not converge. Theoretical arguments indicate that $|\Delta\sigma/\nu|$ should decrease with ν , but they need to be verified. As an example, supposing that $\Delta\sigma = a\nu^b$, the primary goal of the present experiment is to measure b , without the requirement of an accurate measurement of a . Measuring the absolute normalization a is of course beneficial since the determination of b may depend at second order on a . Also to combine the data from this measurement with the world data from ELSA/MAMI/LEGS a must be measured reasonably well, however, this is not the primary objective of this LOI.

The next several sections describe the three main ingredients needed for measuring the polarized yield, which are:

- a beam of circularly-polarized, tagged photons;
- a longitudinally polarized target;
- a large solid-angle detector.

2.1 Beam

Circularly polarized photons are necessary to measure σ_P and σ_A . They can be generated using CEBAF's polarized electrons with an amorphous radiator. Their polarization is [23]:

$$P_\gamma \approx P_e \frac{y(4-y)}{4-4y+3y^2} \quad (2)$$

where $y = \nu/E$ and P_e is the electron beam polarization. P_γ vs y from this the approximate formula in Eq. (2) and from the exact formula are shown on Fig. 2. Also shown is the effect of using different radiator materials for the exact formula. In this proposal P_e is assumed to be 85%. In term of the overall figure of merit, the increase of photon beam

¹barring exotic behaviors such as a singular contribution at $\nu \rightarrow \infty$.

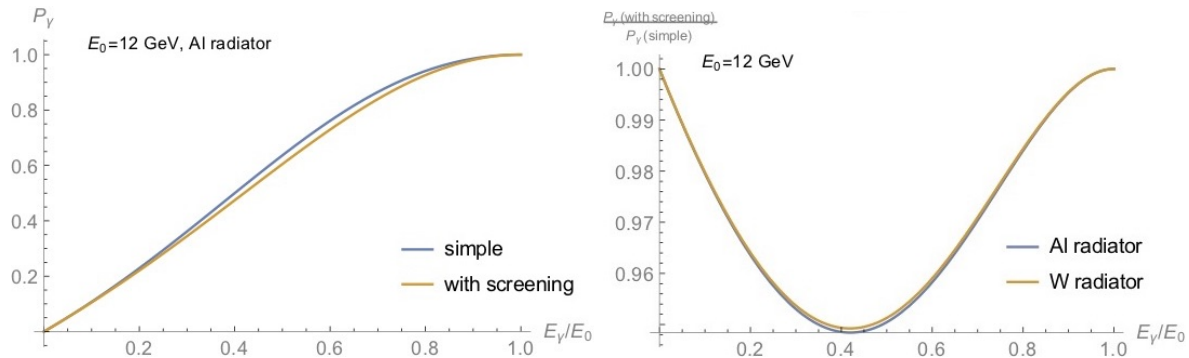


Figure 2: Left: photon circular polarization vs the energy fraction ν/E using the approximate Eq. (2) (blue line), and the exact formula for aluminum material (orange line). Right: ratio between the exact and approximate calculations for different radiator materials (blue: Aluminum; orange: Tungsten.)

polarization at higher ν more than compensates the decreasing flux and cross section. Thus, we expect a better statistical precision at larger ν , see Figs. 3 and 4.

No electron beam polarimetry is presently available in Hall D. Since we are concerned about measuring a yield rather than the absolute determination of $\Delta\sigma$, an accurate polarimetry measurement is not needed. The electron beam longitudinal polarization in Hall D can be measured at 5% level using the injector Mott polarimeter or the polarimeters in Hall A, B or C. The spin precession can be calculated to about 1.2% accuracy for a beam energy known at the 10^{-3} level, the presently known accuracy on the JLab beam energy. Calculations indicate that the depolarization resulting from synchrotron radiation and energy spread are below 1%, which is confirmed by the high beam polarizations measured in Hall A and B at 11 GeV [26].

The photon flux is monitored by the Hall D Pair Spectrometer, calibrated at the few percent level using the Total Absorption Counter, which is more than enough for the present proposal. The Pair Spectrometer covers a momentum range of about 5 GeV. It will thus be necessary to change its magnetic field once or twice during the experimental run to correct the flux for the tagger inefficiency over the full ν -range of the experiment. Changing the Pair Spectrometer field takes less than 10 min.

The photon energy is tagged with a resolution better than 0.5% [27], which again is more than enough for the present proposal.

2.2 Target

Two polarized target systems suited for polarized photons exist at JLab: the HDice and the FROST systems. We assume here that the experiment will run using FROST. The reasons of this choice are:

- HDice has a higher figure of merit than FROST for the proton due to the low HDice target dilution and its ability to sustain a high photon flux. However, the overhead of preparing and installing the target, and its complex operation, make it less suited for a short experiment such as the one discussed here. We expect a 7 days run for each nucleon. Shortening this duration has little benefit to balance the larger work involved with the HDice target.
- The higher dilution of FROST is, in the particular case of experiment discussed here, not a hindrance for two reasons: 1) Any unpolarized material contribution cancels when $\Delta\sigma$ is formed, in contrast to asymmetries or unpolarized cross-section. 2) As we will see in Section 3, the expected DAQ rate is three times smaller than the DAQ system limits. Hence, the extra rate from unpolarized material does not reduce the statistics by requiring the experiment run at lower luminosity due to DAQ limitation.
- Data on polarized neutron need to be taken as well. The significantly higher FROST neutron polarization (80% for FROST vs 25% for HDice) makes FROST a better choice.

However, if there is program of other experiment requiring a polarized target, the choice of HDice may become more pertinent. For now however, we assume that the experiment would run alone, with a FROST target.

2.3 FROST target characteristics

The FROST target makes use of the Dynamical Nuclear Polarization (DNP) technique on butanol (C_4H_9OH or C_4D_9OD). Polarized protons or neutrons (deuterons) can thus be obtained. The target is polarized outside the detector with a 5T field at $T \approx 0.3K$. Its temperature is then lowered to $T \approx 0.03K$ and the target is rolled in position in the main Hall D solenoid which provides a nominal 2 T holding field.

Protons and deuterons reach similar maximum polarization, $P_t > 85\%$. The in-beam polarization relaxation time was about $T_1 \approx 2000$ h (for proton) in CLAS with a 0.5 T

holding field, which will be significantly increased in Hall D under the 2 T solenoid field. The CLAS FROST target had a 0.5% loss per day for positive polarization (1.0% per day for negative polarization.) Its average polarization was 75%, which is the value we assume for P_t in this LOI. In order to reach this average, the target needed to be re-polarized once a week. With the larger 2 T in Hall D, there should be no need to repolarize the target given the expected run time of the present proposal (1 week for the proton run and 10 days for the neutron run). In any case, repolarizing is a 5 h process that can be done opportunistically during the weekly instances when the beam is off for maintenance/development (beam studies or RF recovery). At such occasion, the orientation of the target spin can be reversed in order to have data with the target polarizations parallel and antiparallel to the beam. This allows to minimize potential systematics bias in the measured cross-section asymmetry.

The target cell length would be 5 cm as for the CLAS target, and its diameter 0.7 cm to match the 0.5 cm active collimator size. The target material density (Butanol+ ^4He bath) is 0.66 g/cm 3 for C_4H_9OH and 0.73 g/cm 3 for C_4D_9OD . The solid angle left opened by the target is 75% of 4π but the backward angle coverage can be increased with a new target designed for Hall D [24]. The maximum sustainable photon flux envisioned for a Hall D FROST target will be about 10 times that used with the Hall B FROST target [24], that is about 10^8 γ/s . It can be obtained with a 90 nA beam current on the 2.5×10^{-5} RL radiator. With an additional 0.5 T solenoid around the target nose designed such that the total field uniformity to ≈ 100 ppm, it becomes possible to continuously polarize the target with microwaves and thus not operate it in frozen spin mode. This would increase the maximum sustainable beam flux and 10^9 may be reachable [24]. For this proposal, we assume 10^8 γ/s and the target operating in frozen spin mode. A photon beam hardener that reduces the low energy (< 100 MeV) photon flux, and thus the target heating, can be implemented [25]. Hardeners suppressing the low energy bremsstrahlung photons have been used at SLAC, CEA and DESY.

Two months will be necessary to initially install the target in Hall D and test it. No beam time is needed for its commissioning. To switch from the proton to the deuteron target would take 8 h plus with an additional day to polarize the deuterons, giving a total target change time of 1.5 days. Switching from the deuteron to proton target would take 8 h plus a few hours to polarized the protons, so about 0.5 day. Hence, in this context, it is somewhat advantageous to start the program with the deuteron run.

2.4 Detectors and acquisition

Hall D is the best suited hall at JLab to measure the total photoproduction cross-section thanks to its large solid angle. The standard Hall D detector package plus the PrimEx- η Compton Calorimeter is assumed. Drift chambers are not required except if the asymmetry method is used to obtain the absolute $\Delta\sigma$ necessary to achieve the secondary goals of the proposal. In that case, the asymmetry dilution by unpolarized target material –such as windows– must be corrected for, and vertex reconstruction would thus be beneficial. The calorimeters provide detection of neutral and charged particles over polar angles from 0.2° to 145° with a nearly complete azimuthal coverage. Charged particles are detected by the Forward and Central Drift Chambers (FDC and CDC). Neutral particles are detected by the Forward Calorimeter (FCAL) between 1° and 12° and the Barrel Calorimeter (BCAL) between 12° and 160° . The Compton Calorimeter covers forward angles down to 0.2° . For high beam energies most particles are produced in the forward region, thus good forward angle coverage is critical, while backward angle coverage is less so. The largest angles will be blocked by the target equipment: angles larger than 135° would be blocked if the Hall B FROST target is used. We assume that the Hall D target will permit detection up to 160° .

The Hall D solid angle can be compared to the 7° to 145° polar angle coverage of the LEGS detector at BNL and to the 1.6° to 174° polar angle coverage of the GDH-detector at ELSA. The LEGS procedure to correct for the missing forward (and, less importantly, backward) angular coverage was to use their PWA analysis results to constrain the $\Delta\sigma$ extrapolation. This method appeared to yield a robust correction [20].

The $120 \mu\text{b}$ total γp unpolarized cross section and 5 cm target of density 0.66 g/cm^3 (proton) or 0.73 g/cm^3 (deuteron) yield total rates of 36 kHz or 40 kHz, respectively², well below the current 60 kHz DAQ limit of Hall D. Hence, there will be no significant deadtime or other limitation from the DAQ system.

3 Sensitivity and beam time request

To estimate the beam time necessary for the measurement, we use a total collimated photon flux of $1 \times 10^8 \text{ s}^{-1}$. It can be obtained with the Hall D 2×10^{-5} RL aluminum radiator ($1.6 \mu\text{m}$), 50 nA electron beam current and the 5 mm Hall D collimator. The tagged flux between $\nu = 3$ and 12 GeV represents 25% of the total flux,

²The dilution factor of butanol is about $10/74=0.135$ (proton) or $20/84=0.238$ (deuteron), which yield a useful rate of 5 kHz and 10 kHz, respectively.

thus a $2.5 \times 10^7 \text{ s}^{-1}$ flux is used to determine the interaction rate. 80% is assumed for the detector efficiencies, 75% for the available solid angle from the target, 85% for the electron beam polarization. 75% H and D target polarizations. For $\Delta\sigma$, we use the Regge form

$$\sigma_P - \sigma_A = I c_1 s^{\alpha_{a_1} - 1} + c_2 s^{\alpha_{f_1} - 1}, \quad (3)$$

with $s = 2M\nu + M^2$, $I = \pm$ is the isospin sign of the proton or neutron and assumed values for the following constants $c_1 = -34.1 \text{ } \mu\text{b}$, $\alpha_{a_1} = 0.42$, $c_2 = 209.4 \text{ } \mu\text{b}$, $\alpha_{f_1} = -0.66$ [2].

If $\Delta\sigma$ indeed follows Eq. (3), then running 7 days on the proton target and 10 days on the deuteron target yields a similar statistical precision for the neutron and proton data as shown in Figs. 3 and 4, respectively. The expectation for the deuteron (from which the neutron results are determined) is shown in Fig. 6. These precise measurements will provide the inputs needed to separate the different isospin components, as shown in Fig. 5.

This simulation yields uncertainties on the intercepts of $\Delta\alpha_{a_1} = \pm 0.006$ and $\Delta\alpha_{f_1} = \pm 0.016$ to be compared with the values $\Delta\alpha_{a_1} = \pm 0.23$ and $\Delta\alpha_{f_1} = \pm 0.22$ extracted from the ELSA data [2]. We are comparing here to results from the best fit to the photoproduction data. The intercept values can also be obtained from low- Q^2 electroproduction data, and with higher precision, see e.g. the recent determination $\alpha_{a_1} = 0.31 \pm 0.04$ Ref. [12]. However, systematics uncertainties are associated with such extraction, in particular regarding what should be the highest Q^2 values acceptable for Regge-type fit, and the assumption that the data are Q^2 -independent. Thus, our projected results are expected to significantly improve, statistically and systematically, over values derived from previous photoproduction and low- Q^2 electroproduction results.

3.1 Uncertainties

Since we are primarily interested in the high- ν behavior of the yield difference $N^+ - N^-$, and since the data at various ν are taken concurrently, an accurate absolute normalization of $\sigma_P - \sigma_A$ is of secondary importance. However, such an absolute normalization is necessary in order to accurately compute the high energy contribution of the GDH sum. The absolute normalization can be obtained by measuring the asymmetry $A = (N^+ - N^-)/(N^+ + N^-)$ and use the well measured unpolarized cross-section σ_0 to obtain $\Delta\sigma = 2\sigma_0 A$. For the purpose of normalization, A needs not be measured over the full ν coverage. Thus for this ancillary goal, we assume the following values for uncertainties:

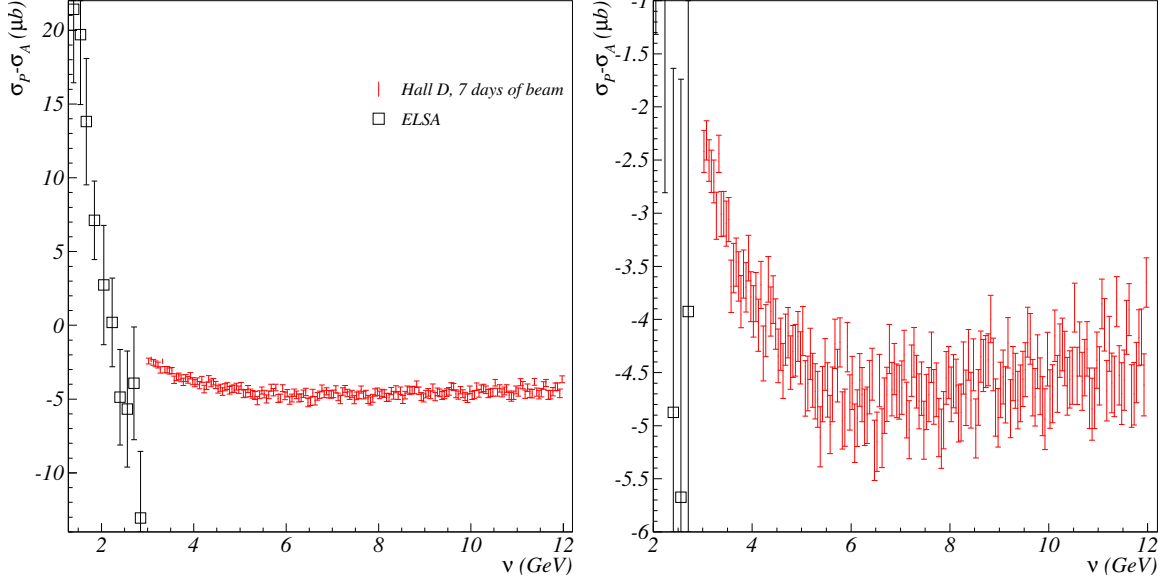


Figure 3: Left: $\Delta\sigma$ on the proton from ELSA high- ν data and expected results from Hall D. Right: Same as left, but zoomed on the expected Hall D data. The line is a fit to simulated data based on the Regge form Eq. (3). The parameters $\alpha_{a_1} = 0.406 \pm 0.006$ and $\alpha_{f_1} = -0.694 \pm 0.028$ are the best values for the Regge intercepts of the a_1 and f_1 meson trajectories.

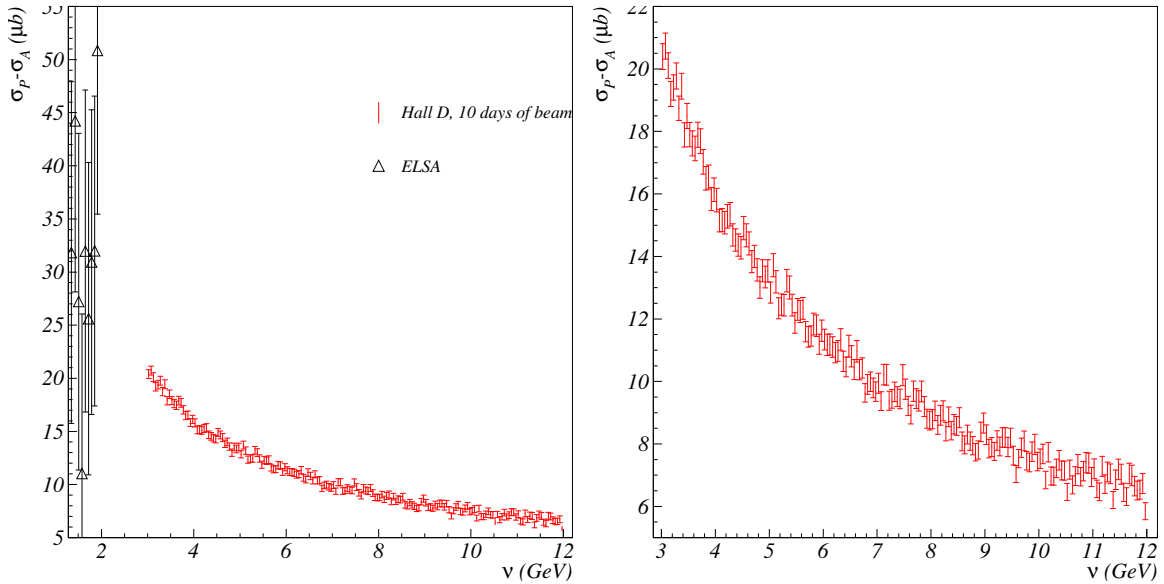


Figure 4: Same as Fig. 3, but for the neutron extracted from deuteron data. The best values for the Regge intercepts of the a_1 and f_1 meson trajectories are $\alpha_{a_1} = 0.388 \pm 0.010$ and $\alpha_{f_1} = -0.558 \pm 0.038$.

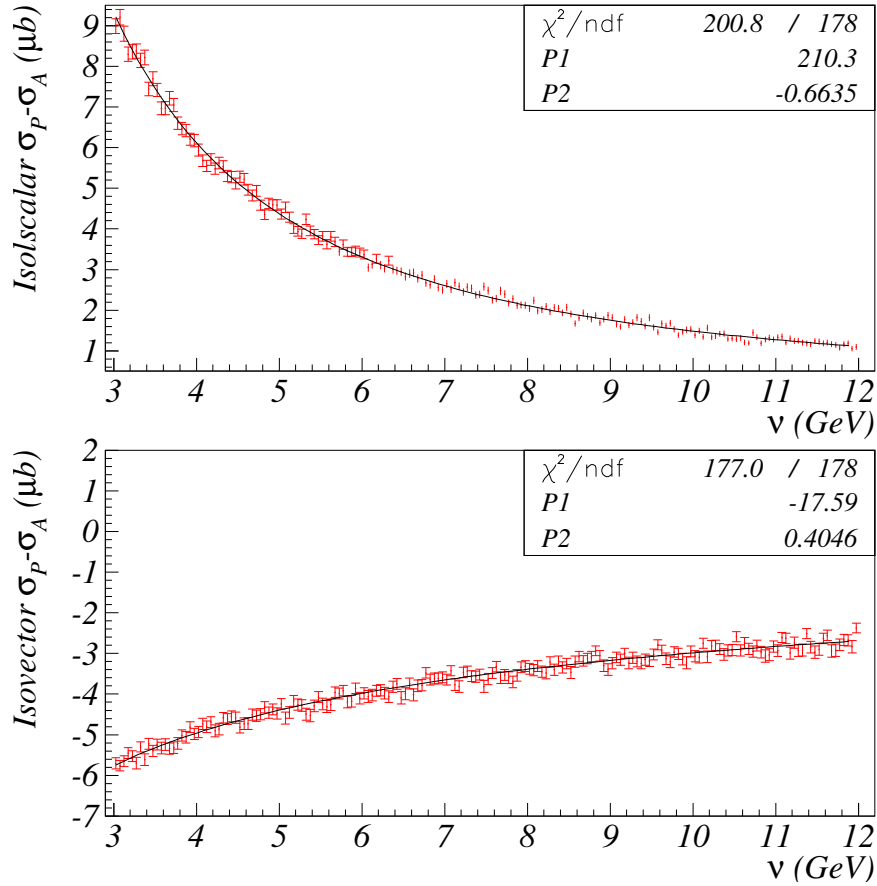


Figure 5: Isospin decomposition of $\Delta\sigma$. Top: isoscalar part, with best value for the Regge intercepts of the f_1 meson trajectory $\alpha_{f_1} = -0.664 \pm 0.016$. Bottom: isovector part, with best value for the Regge intercepts of the a_1 meson trajectory $\alpha_{a_1} = 0.405 \pm 0.008$.

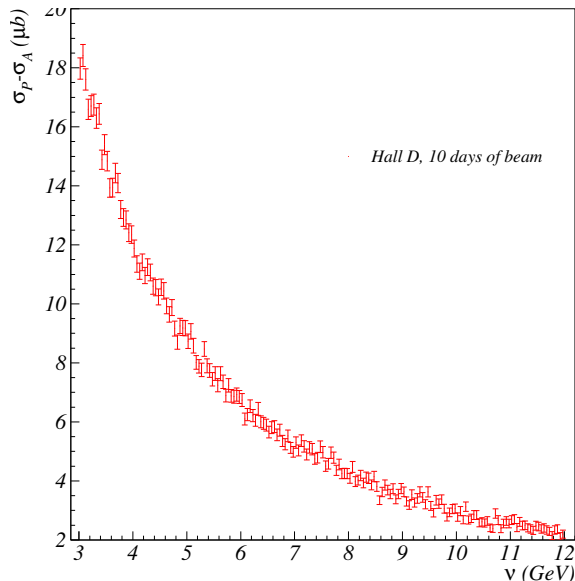


Figure 6: $\Delta\sigma$ for the deuteron expected results from Hall D. The best fit to these simulated data is $\Delta\sigma = 421(7)s^{-1.663(7)}$

- Beam polarization: $\Delta P_e = 4\%$, with 2% due to precession and knowledge of beam energy, 1% due synchrotron radiation depolarization and 3% from Mott/Hall polarimeters.
- Target polarization: $\Delta P_t = 3\%$.
- Target dilution: $\Delta D = 3\%$.
- Unpolarized cross-section σ : $\Delta\sigma_0 = 1\%$.

Carbon data for target dilution will need to be taken separately with a solid target. This target can be mounted within 8h. We assume 1 day of data taking. Alternatively, $\Delta\sigma$ could be computed directly, although presumably with significantly larger uncertainties. In that case Carbon data would be unnecessary.

A third possibility to normalized the yield difference would be to run a day on the proton with an electron beam energy of 9 GeV, providing an overlap in the photon beam energy with previous measurements from ELSA/MAMI. This would provide an important cross-check and an absolute normalization of our cross-sections. However, since Hall D utilizes the highest energy provided by CEBAF this would require coordination with the physics programs in the other Halls and we assume 2 days of configuration change for CEBAF to run at this lower energy.

In all, these systematic contributions represent a total systematic uncertainty of 6%. The statistical uncertainty is negligible compared to this systematic contribution. Since the high-energy contribution to the GDH sum rule is expected to represent about 6% of the total sum rule, assuming the validity of the sum rule, the measurement will improve by 25% the precision at which the the GDH sum rule for the proton is tested. Specifically, it will decrease the total systematic uncertainty of the world data from 16 μb to 12 μb .

4 Impact of the results

Beside studying the convergence properties of the GDH sum rule in the relevant (i.e. high- ν) domain, the proposed $\Delta\sigma(\nu)$ data at high- ν will improve our knowledge on both the imaginary and real parts of the spin-dependent Compton amplitude f_2 ; it will provide new information on the little known intercept of the a_1 Regge trajectory; it will yield the first non-zero polarized deuteron asymmetry in the diffractive regime, thereby providing for the first time a non-zero value for the isosinglet coefficient of $\Delta\sigma$; it will reduce the uncertainty of the polarizability contribution to $1S$ hyper-fine splitting in muonic hydrogen; and it will provided a photon-point benchmark to study the transition between the well-understood DIS dynamics of QCD to the lesser-known dynamics of diffractive scattering that will be explored with the EIC [28]. We also discuss quantitatively what we would learn if the GDH sum rule is found to violated, using the example of quark compositeness. These six items are discussed separately in the following sections.

4.1 Determination of the real and imaginary parts of the spin-dependent Compton amplitude $f_2(\nu)$

The spin-dependent Compton amplitude $f_2(\nu)$, also denoted by $g(\nu)$ in literature, is a complex quantity whose imaginary part is determined by $\Delta\sigma$ using dispersion relation and will thus be measured directly by the experiment. Fig. 7 (top) shows the world data on $\Im m(f_2)$ extracted from $\Delta\sigma$ measured at MAMI and ELSA.

The real part, $\Re e(f_2)$, is obtained from $\Im m(f_2)$ by a standard dispersion relation [29]. The reliability of this extraction is shown by the violet error band in Fig. 7, and strongly depends on the quality of $\Im m(f_2)$ (blue error band). If both $\Re e(f_2)$ and $\Im m(f_2)$ were

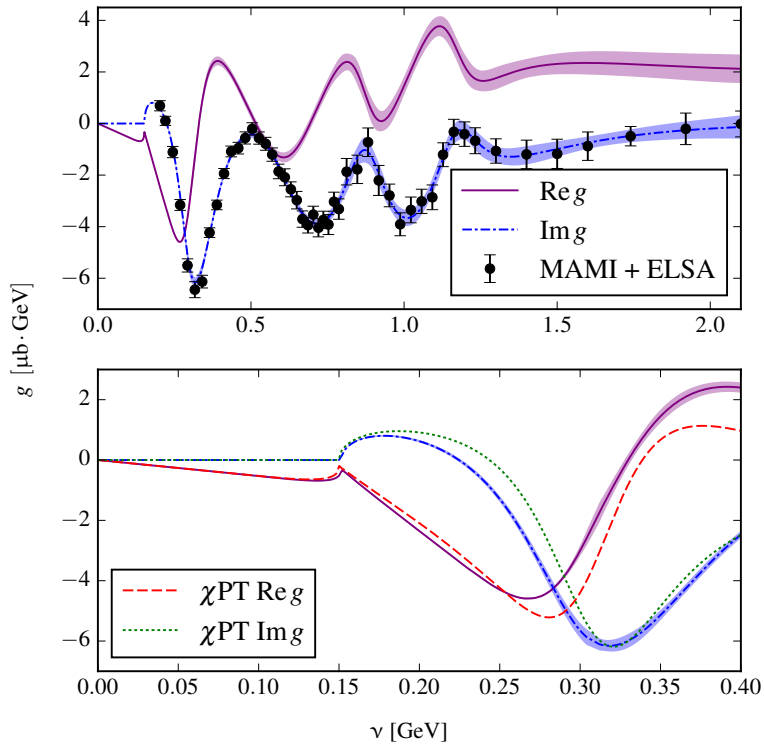


Figure 7: The spin-dependent Compton amplitude $f_2(\nu)$, denoted g in the figure. Top: real and imaginary parts, the latter fitted to GDH data, the former calculated via dispersion relations. Bottom: χEFT calculation. Figure from [30].

known precisely enough (and given f_1 , which is well measured), the two complex amplitudes could be used to determine $d\sigma/d\Omega$ and the beam-target asymmetry Σ_{2z} in the forward limit, i.e.,

$$\left. \frac{d\sigma}{d\Omega} \right|_{\theta=0} = |f_1|^2 + |f_2|^2, \quad \Sigma_{2z}|_{\theta=0} = -\frac{f_1 f_2^* - f_1^* f_2}{|f_1|^2 + |f_2|^2},$$

The latter quantity is most interesting since the asymmetry for circularly polarized photons and nucleons polarized along the z axis,

$$\Sigma_{2z} = \frac{d\sigma_P - d\sigma_A}{d\sigma_P + d\sigma_A},$$

provides information on all four spin polarizabilities appearing in Compton scattering. In particular Σ_{2z} and its behavior near $\theta = 0$ are very sensitive to chiral loops [31]. The product of the unpolarized cross-section and Σ_{2z} for $\theta = 0$ is shown in Fig. 8 (top) together with its uncertainty, which increases rapidly for $\nu \gtrsim 2$ GeV. Thus, the precise measurement of $\Delta\sigma(\nu)$ in the ν range covered in Hall D will significantly reduce the uncertainty on Σ_{2z} .

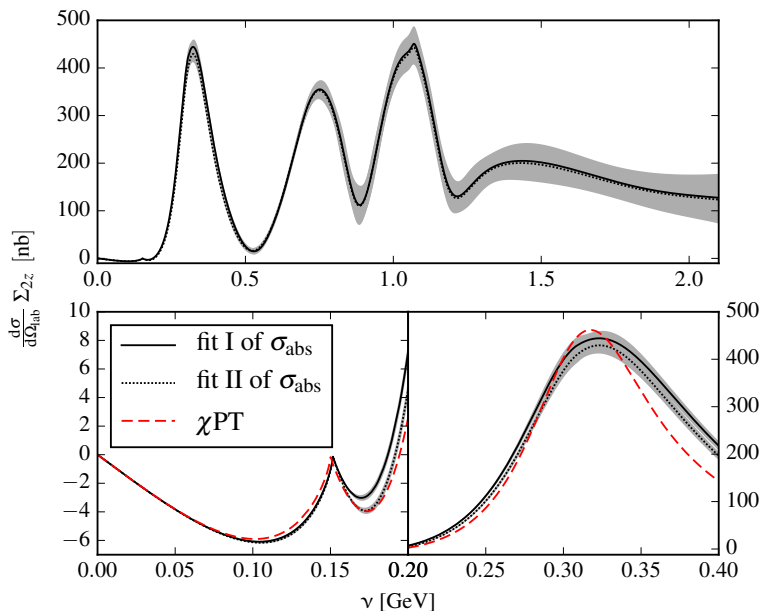


Figure 8: Unpolarized differential cross section multiplied with the Σ_{2z} asymmetry for the forward Compton scattering off the proton, showing (top) two distinctive fits of the unpolarized photoabsorption cross section and its uncertainties, and (bottom) the χ EFT calculation. Figure from [30].

Chiral effective field theory (χ EFT) is an important non-perturbative effective ap-

proach to QCD that should describe it at low energy-momentum. However, the dedicated JLab low Q^2 experimental program to test χ EFT with spin observables is showing that their description is a challenge to χ EFT [6]. Thus, providing further tests of χ EFT with new spin observables or/and in a different regime is critical and can be achieved with the present proposal.

4.2 The intercept of the a_1 Regge trajectory

In Regge theory, the high-energy behavior of the isovector (non-singlet) and isoscalar (singlet) cross-section differences are driven by the $a_1(1260)$ and $f_1(1285)$ Regge trajectories such that

$$\Delta\sigma^{(p-n)} \sim s^{\alpha_{a_1}-1}, \quad \Delta\sigma^{(p+n)} \sim s^{\alpha_{f_1}-1},$$

where typically $\alpha_{a_1} \approx 0.4$ and $\alpha_{f_1} \approx -0.5$ as obtained from fits to DIS data. A very recent such fit [32] resulted in $\alpha_{a_1}^{\text{DIS}} \approx +0.45$ and $\alpha_{f_1}^{\text{DIS}} \approx -0.36$, while the Regge expectations are $\alpha_{a_1} \approx -0.34$ and $\alpha_{f_1} \approx -0.45$ (see e.g. Eq. (4)). Another recent fit, combining both electroproduction and photoproduction data [12], yields $\alpha_{a_1}^{\text{DIS},\gamma} = +0.31 \pm 0.04$, i.e. also finds that the sign of the $a_1(1260)$ intercept is opposite to the theoretical prediction. The problem at the root of the discrepancy on α_{a_1} is partly that $a_1(1260)$ is the only $I^G(J^{PC}) = 1^-(1^{++})$ meson to form a ‘‘trajectory’’, while the second candidate, the $a_1(1640)$, has been omitted from the PDG Summary Tables as it still needs confirmation. A precise measurement of $\Delta\sigma$ at high ν for both proton and neutron targets would help to remove this uncertainty. This is an important question to resolve as the intercept is given by

$$\alpha_{a_1} = 1 - \alpha' m_{a_1}^2, \tag{4}$$

where $\alpha' = 1/(2\pi\sigma) \approx 0.88 \text{ GeV}^{-2}$ and σ is the string tension, which is known to be approximately 0.18 GeV^2 . If α_{a_1} were indeed ≈ 0.45 , this would imply $\alpha' \approx 0.44 \text{ GeV}^{-2}$ and a string tension more than twice as high as the commonly accepted value.

As discussed in Section 3, if $\Delta\sigma$ obeys the presumed Regge behavior, the experiment would determine the Regge intercepts at the level of 1.4% for α_{a_1} and 2.4% for α_{f_1} . This represents an improvement in precision of a factor of 36 for α_{a_1} and of 14 for α_{a_1} compared to the world data, from which they are known (54% for α_{a_1} and 33% for α_{f_1}) [2].

4.3 Deuteron asymmetry

Since only null asymmetries have been measured by COMPASS, CLAS and SLAC for the deuteron in the low Q^2 , high- ν , regime relevant to Regge theory, the deuteron coefficient N_1^0 that factors the s -dependence of $\Delta\sigma^{p+n}$ is assumed to be zero in analyses [11, 12]. A non-zero deuteron asymmetries, i.e. $\Delta\sigma^{p+n} \neq 0$, should be clearly measured by this experiment, see Fig. 6, yielding a clear non-zero coefficient for the s -dependence of $\Delta\sigma^{p+n}$, $N_1^0 = -421 \pm 7$, providing that Regge theory describes the data and that the ELSA and DIS fits are relevant to the present regime.

4.4 Polarizability correction to hyperfine splitting in muonic hydrogen

A third impact of the measurement concerns the “proton radius puzzle” [33], specifically to the effect of proton structure on the hyperfine splitting in muonic hydrogen,

$$E_{\text{HFS}}(nS) = [1 + \Delta_{\text{QED}} + \Delta_{\text{weak}} + \Delta_{\text{structure}}] E_{\text{Fermi}}(nS) .$$

The proton-structure correction can be split into three terms: the Zemach radius, the recoil contribution, and the polarizability contribution,

$$\Delta_{\text{structure}} = \Delta_Z + \Delta_{\text{recoil}} + \Delta_{\text{pol}} .$$

The current relative uncertainties of the three terms are 140 ppm, 0.8 ppm and 86 ppm, respectively, which need to be put into the perspective of the forthcoming PSI measurement of E_{HFS} whose precision is expected to be as low as 1 ppm. Our proposed measurement can contribute to the uncertainty reduction of Δ_{pol} . It can be written as

$$\Delta_{\text{pol}} = \frac{Z\alpha m}{2\pi(1+\kappa)M} [\delta_1 + \delta_2] .$$

Here δ_1 involves an integral of the spin structure function $g_1(x, Q^2)$ over both x and Q^2 , while δ_2 involves a similar integration of $g_2(x, Q^2)$ [29]. Since g_1 at low Q^2 is essentially the GDH integrand,

$$\Delta\sigma = \frac{4\pi\alpha^2}{m\mathcal{F}} \left(g_1 - \frac{Q^2}{\nu^2} g_2 \right) ,$$

a precise measurement of $\Delta\sigma$ would constrain δ_1 . To calculate δ_1 , one indeed needs the Q^2 dependence of g_1 , but the integrand being weighted by $1/Q^3$, knowing the value at

$Q^2 = 0$ is critical to stabilize the integration. Such a stabilization is essential, as the mentioned 86 ppm uncertainty needs to be reduced to ≈ 1 ppm. This implies that our knowledge of g_1 needs to be improved by two orders of magnitude.

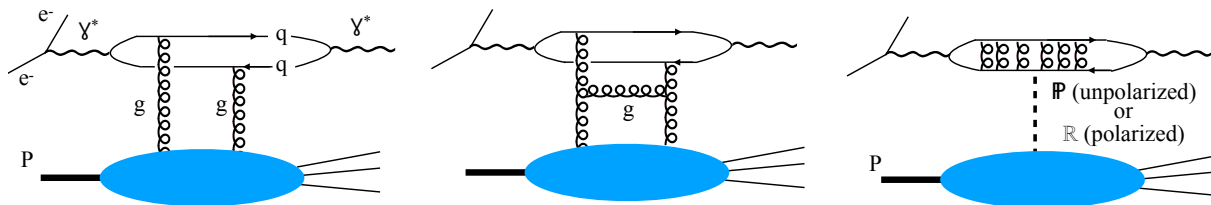


Figure 9: Diquark picture of low- x electron-proton scattering, from the higher Q^2 hard regime (left) to the low Q^2 soft regime with Pomeron or Reggeon exchange (right).

4.5 Transition between polarized DIS to diffractive regimes

As already quoted from Ref. [10], “above the resonance region [...] the real photon is essentially absorbed by coherent processes, which require interactions among the constituents such as gluon exchange between two quarks. This behavior differs from DIS, which refers to incoherent scattering off the constituents.” That is there is a transition between the DIS regime and the very low- x or real photon regimes of diffractive scattering. Studying this transition has been an important part of the ZEUS and H1 programs at HERA, and it remains a very active field of research. However, it is currently limited to unpolarized scattering. The polarized case and its connection to photoproduction is discussed in Ref. [11] and will be explored with the EIC [28].

The traditional theoretical description of diffractive scattering is the diquark picture: the hard virtual photon emitted by the scattered lepton hadronizes into a $q\bar{q}$ pairs of coherent length $1/(xM_p)$. At high enough Q^2 , each quark exchanges a gluon with the proton, see Fig. 9, left panel. As Q^2 decreases, gluons rungs on the gluon ladder appear (Fig. 9, central panel), as well as gluons exchanged between the q and \bar{q} . At very low Q^2 , the interaction between the coherent $q\bar{q}$ pair and the proton is summed into Pomeron \mathbb{P} and Reggeon \mathbb{R} exchanges (Fig. 9, right panel). Other processes contributing to \mathbb{P} and \mathbb{R} exchanges exist, such as the one shown in Fig. 10. This picture connects to the usual DIS parton model, e.g. with the gluons of Fig. 9’s left panel representing the gluon PDF. The Pomeron has the vacuum quantum numbers (isoscalar charge singlet). Thus, its spin 0 makes \mathbb{P} to couple to the proton components irrespective of their helicity.

\mathbb{P} thus controls unpolarized diffractive scattering. In contrast, doubly polarized e^+P scattering filters out \mathbb{P} exchange to reveal the non-singlet \mathbb{R} exchange. This filter will be used for the first time at the EIC. The proposed measurement of $\Delta\sigma$, expected to be also controlled by Regge theory, will provide a $Q^2 = 0$ baseline to this study of the

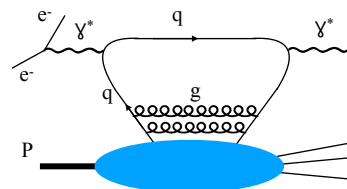


Figure 10: $\vec{e}^+ \vec{P}$

transition from hard dipole partonic picture to the soft \mathbb{R} exchange picture.

4.6 Constraint on quark compositeness or size

Compositeness of quarks implies that they have non-zero anomalous magnetic moments κ_q . Another contribution to κ_q comes from the cloud of gluons and $q\bar{q}$ pairs around the current quark. This contribution is interpreted as the anomalous magnetic moment of the (non-pointlike) constituent quark. However, this contribution is not relevant for two reasons:

1. Above the constituent quark scale, current quarks are resolved. Only perturbative effects analogous to the electron Schwinger moment contribute to κ_q , and it has been shown that the GDH sum rule is valid within perturbation theory [3].
2. The anomalous magnetic moments of constituent quarks would not violate the sum rule since reactions involving them contribute to the final states summed in the GDH inclusive integral. Specifically, such reactions contribute to the non-resonant background present underneath resonance reactions [3].

Thus, unless non-perturbative effects exist at the resolution scale covered by the experiment, the anomalous magnetic moment κ_q of constituent quarks can be ignored: only the $\kappa_q \neq 0$ of current quarks are relevant to a possible violation of the sum rule.

With $\kappa_q \neq 0$, the proton GDH sum rule is modified as [7, 3]:

$$4\pi^2\alpha \left(\frac{\kappa_p^2}{2M_p^2} - \tilde{g}_a \right) = \int_{\nu_0}^{\infty} \frac{\Delta\sigma(\nu)}{\nu} d\nu, \quad (5)$$

with κ_p the anomalous moment of the proton, M_p its mass, and $\tilde{g}_a \approx 1.8 \frac{\kappa_u^2}{2m_u^2}$, with κ_u the u quark anomalous moment and m_u its mass. Other quarks contribute to less than 10% to \tilde{g}_a due to their higher masses and the dominance of the u quark in the proton.

Knowing the validity of the GDH sum rule within 6% implies $\left(\frac{\kappa_u^2 M_p^2}{1.8\kappa_p^2 m_u^2} \right) \lesssim 6\%$. At the 2 GeV scale and in the \overline{MS} scheme, $m_u = 2.2_{-0.4}^{+0.5}$ MeV [5]. Taking 7 GeV as the typical scale of the proposed experiment, the running mass evolves to $m_u = 1.7$ MeV [34]. This yields $M_p/m_u = 550$ and $\kappa_u \lesssim 2.5 \times 10^{-4} \kappa_p$. The simplest interpretation³ is that this

³Based on dimensional analysis: $[\kappa] = e \cdot \text{fm}$. The electric charge e evidently does not enter the scaling, e.g. the neutron anomalous magnetic moment is non-zero. This simple scaling is also suggested by the fact that the ratio $\kappa_p/r_p^m \approx |\kappa_n|/r_n^m = 1.036$ is nearly unity. (r_p^m and r_n^m are the proton and neutron magnetic radii, respectively.)

constraint translates the 0.25 GeV (or magnetic radius $r_p^m = 0.78$ fm) proton size into a 1.0 TeV (or 2.1×10^{-4} fm) constraint on the size of the quark. Smaller uncertainties in the resonance part of the sum rule provided by the very low Q^2 proton data of the CLAS EG4 experiment, as done in [35], and the possibility that the u quark mass could be lighter (1.4 MeV at 7 GeV) could push this constraint to 10^{-4} fm, or 2 TeV.

The fact that this experiment could probe quark compositeness at a much higher scale than JLab energy is not surprising: the anomalous magnetic moment is a very sensitive tool to probe compositeness, as illustrated by the fact that the discovery of the proton anomalous magnetic moment (1930) largely predates the direct evidence for nucleon compositeness from high-energy electron scattering (1957).

5 Summary

We propose the first measurement of the high-energy behavior of the integrand $\Delta\sigma/\nu$ of the GDH sum rule, a fundamental relation of quantum field theory whose validity depends on the internal dynamical properties of the particle on which the sum rule is applied. The measurement would take place in Hall D, using the FROST target and a polarized beam on a Al. radiator. The high- ν domain probed by this measurement is sensitive to possible violations of the sum rule. In fact, the unpolarized equivalent of the GDH integral does not converge, both for the proton and the neutron, which was made clear only from high- ν data, $\nu > 3$ GeV, which is greater than the energy range covered by previous measurements of the GDH integrand. The proposed measurement, up to $\nu = 12$ GeV, would provide critical input on the convergence of the GDH sum rule.

The first goal of the experiment is to map with high precision the energy dependence $\Delta\sigma$ on the proton and neutron. This will determine whether $\Delta\sigma$ follows the expected Regge behavior and if so, the values of the isovector and isoscalar intercepts will determine if the sum rule converges. Only point-to-point uncorrelated errors contribute to the intercept uncertainties. Assuming 3 weeks of measurement (one week on proton, 10 days on deuteron, 1 days for target dilution measurements and 2 days at lower LINAC energy to overlap with the MAINZ/ELSA data) and a Regge behavior will provide the intercepts at the 2% level, compared to the 50% uncertainties at which they are presently known.

In all, three weeks of beam time are needed to reach these goals. An additional 12h is needed to switch from the deuteron to proton target (or 36 hours if the experiment starts on the proton) and another 8h to install a carbon target for a polarized target dilution measurement. Once a polarized target is available in Hall D, a rich experimental program will open [36]. It is sensible to initiate it with the simplest experiment and a robust observable.

References

- [1] S. B. Gerasimov, Sov. J. Nucl. Phys. **2**, 430 (1966) [Yad. Fiz. **2**, 598 (1965)]; S. D. Drell and A. C. Hearn, Phys. Rev. Lett. **16**, 908 (1966); M. Hosoda and K. Yamamoto Prog. Theor. Phys. **36** (2), 425 (1966).
- [2] K. Helbing, Prog. Part. Nucl. Phys. **57**, 405 (2006) [nucl-ex/0603021].
- [3] R. Pantforder, hep-ph/9805434.
- [4] S. D. Bass, Mod. Phys. Lett. A **12**, 1051 (1997) [hep-ph/9703254].
- [5] M. Tanabashi *et al.* [Particle Data Group], Phys. Rev. D **98**, 030001 (2018).
- [6] A. Deur, S. J. Brodsky and G. F. De Tera mond, Rep. Prog. Phys. arXiv:1807.05250
- [7] K. Kawarabayashi and M. Suzuki, Phys. Rev. **152**, no. 4, 1383 (1966); A. Khare, Prog. Theor. Phys. **53**, 1798 (1975); J. L. Friar, Phys. Rev. C **16**, 1504 (1977); M. De Sanctis, D. Drechsel and M. M. Giannini, Few Body Syst. **16**, 143 (1994).
- [8] H. D. I. Abarbanel and M. L. Goldberger, Phys. Rev. **165**, 1594 (1968).
- [9] L. N. Chang, Y. g. Liang and R. L. Workman, Phys. Lett. B **329**, 514 (1994) [hep-ph/9403286].
- [10] D. Drechsel and T. Walcher, Rev. Mod. Phys. **80**, 731 (2008) [arXiv:0711.3396 [hep-ph]].
- [11] S. D. Bass and A. De Roeck, Eur. Phys. J. C **18**, 531 (2001) [hep-ph/0008289].
- [12] S. D. Bass, M. Skurzok and P. Moskal, Phys. Rev. C **98**, no. 2, 025209 (2018) [arXiv:1808.03202 [hep-ph]].
- [13] O. R. Frisch and O. Stern Z. Physik **85**, 4-16 (1933) I. Estermann, O. R. Frisch, O. Stern Nature **132**, 169-170 (1933)
- [14] R. Hofstadter, Ann. Rev. Nucl. Part. Sci. **7**, 231 (1957).
- [15] J. D. Bjorken, NATO Sci. Ser. B **197**, 1 (1987).
- [16] P. Bosted *et al.* SLAC E159, proposal
- [17] J.P. Chen *et al.* CLAS proposal E94-117

- [18] S. D. Bass and M. M. Brisudova, *Eur. Phys. J. A* **4**, 251 (1999) [hep-ph/9711423];
- [19] R. de L. Kronig, *J. Opt. Soc. Am.*, vol. 12, pp. 547-557 (1926); H. A. Kramers, *Atti Cong. Intern. Fisica*, (Transactions of Volta Centenary Congress) Como, vol. 2, p. 545-557 (1927).
- [20] S. Hoblit *et al.* [LSC Collaboration], *Phys. Rev. Lett.* **102**, 172002 (2009), [arXiv:0808.2183 [hep-ex]].
- [21] J. Ahrens *et al.* [GDH and A2 Collaborations], *Phys. Rev. Lett.* **87**, 022003 (2001), [hep-ex/0105089]; H. Dutz *et al.* [GDH Collaboration], *Phys. Rev. Lett.* **91**, 192001 (2003); *Phys. Rev. Lett.* **93**, 032003 (2004);
- [22] D. Drechsel, O. Hanstein, S. S. Kamalov and L. Tiator, *Nucl. Phys. A* **645**, 145 (1999) [nucl-th/9807001]; *Phys. Rev. D* **63**, 114010 (2001) [hep-ph/0008306].
- [23] H. Olsen and L. C. Maximon, *Phys. Rev.* **114**, 887 (1959).
- [24] C. Keith. Personal communication.
- [25] . B. F. Stearns, *Review of Scientific Instruments* 36, 548 (1965)
- [26] J. Grames. Personal communication.
- [27] A. Somov. Personal communication.
- [28] A. Accardi *et al.*, *Eur. Phys. J. A* **52**, 268 (2016) [arXiv:1212.1701 [nucl-ex]].
- [29] F. Hagelstein, R. Miskimen, V. Pascalutsa, *Prog. Part. Nucl. Phys.* **88** (2016) 29.
- [30] O. Gryniuk, F. Hagelstein, V. Pascalutsa, *Phys. Rev. D* **94** (2016) 034043.
- [31] V. Lensky, J. A. McGovern, V. Pascalutsa, *Eur. Phys. J. C* **75** (2015) 604.
- [32] M. Vanderhaeghen, private communication.
- [33] For a review, see R. Pohl, R. Gilman, G. A. Miller and K. Pachucki, *Ann. Rev. Nucl. Part. Sci.* **63**, 175 (2013) [arXiv:1301.0905 [physics.atom-ph]].
- [34] H. Fusaoka and Y. Koide, *Phys. Rev. D* **57**, 3986 (1998) [hep-ph/9712201].
- [35] K. P. Adhikari *et al.* [CLAS Collaboration], *Phys. Rev. Lett.* **120**, no. 6, 062501 (2018) arXiv:1711.01974 [nucl-ex].
- [36] D. Keller *et al.* Target Helicity Correlations in GlueX. JLab LOI12-16-005.